

First loosely coherent all-sky search for periodic gravitational waves in the O1 LIGO data.

Vladimir Dergachev^{1,2, a} and Maria Alessandra Papa^{1,2, b}

¹Max Planck Institute for Gravitational Physics (Albert Einstein Institute), Callinstrasse 38, 30167 Hannover, Germany

²Leibniz Universität Hannover, D-30167 Hannover, Germany

A new loosely coherent analysis improves sensitivity to continuous gravitational waves by more than 30%, with order of magnitude gains in computational efficiency. Results of all-sky search in 20-200 Hz frequency band are provided including outlier lists and upper limits near 0-spindown band suitable for analysis of signals with small spindown such as boson condensates around black holes.

We report the results (Figure 1) of first all-sky loosely coherent search [1–3] for continuous gravitational waves in data from LIGO’s first observation run (O1) [4–6]. The search covers 20-200 Hz frequency band and frequency derivative (spindown) from -1×10^{-8} through 1.11×10^{-9} Hz/s.

Loosely coherent algorithms [1–3] are designed to explore parameter spaces covered by large template banks by searching many nearby templates at once. The ability to perform an all-sky search using loosely coherent algorithm marks an important breakthrough in scalability of these methods.

Previously published wide-parameter searches include Einstein@Home, PowerFlux, Frequency Hough, Sky Hough, and Time domain F-statistic [7–9]. These searches iterate over template banks covering sky, frequency and other parameters. PowerFlux has used loosely coherent methods for outlier followup. Previously published PowerFlux data provided the most sensitive upper limits above 100 Hz and is the only search to offer worst-case 95% confidence level upper limits.

Compared with previously published PowerFlux data the loosely coherent upper limit is further reduced by more than 30% (Figure 2) increasing the search volume by 190%. In order to achieve this sensitivity the previous PowerFlux search [8, 9] would have needed a factor of 4 larger the coherence time, with computation time growing by a factor of hundreds. This extrapolation assumes that upper limits are inversely proportional to the fourth root of the coherence time, given a fixed amount of data [1, 10, 11]. Since the maximum coherence time in the PowerFlux search is limited by the Doppler shifts from Earth rotation, such hypothetical search could not be carried out.

In the frequency band 100-200 Hz these results are the most sensitive to date. At the high end of the frequency range we are sensitive to a source with 10^{-6} equatorial ellipticity up to 440 pc away. Below 100 Hz the upper limits are comparable to results from the Einstein@Home search [7], but cover larger spindown range up to 10^{-8} Hz/s.

A comparison between previously established PowerFlux upper limits [8] and new loosely coherent results is shown in Fig. 2. While at high frequencies we reduce the

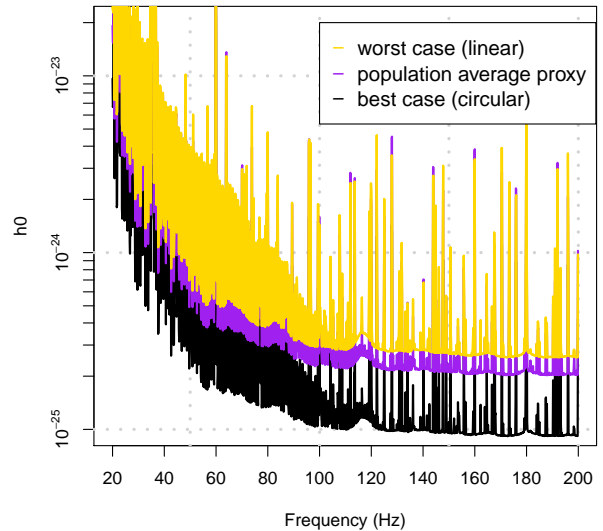


FIG. 1. O1 upper limits. The dimensionless strain (vertical axis) is plotted against signal frequency. Looking at the right side of the plot, the upper (yellow) curve shows worst-case (linear polarization) upper limits, the next lower curve (purple) shows population average proxy, followed by black curve showing upper limits for circularly polarized signals. The worst-case and best-case upper limits are maximized over sky and all intrinsic signal parameters for each frequency band displayed. (color online)

upper limit by 30% or more, below 100 Hz there is a lot of scatter due to 0.25 Hz comb of instrumental lines and other instrumental artifacts [12]. The two codes have different coherence times and show very different response to instrumental disturbances. Following [13] we compute sensitivity depth as square root of power spectral density divided by the upper limit (Table I).

The upper limit data is available in computer readable format in [14]. The upper limits are computed using universal statistic algorithm [15] and are valid in all frequency bands and for the entire sky. The worst case (linear) and circular polarization 95% confidence level

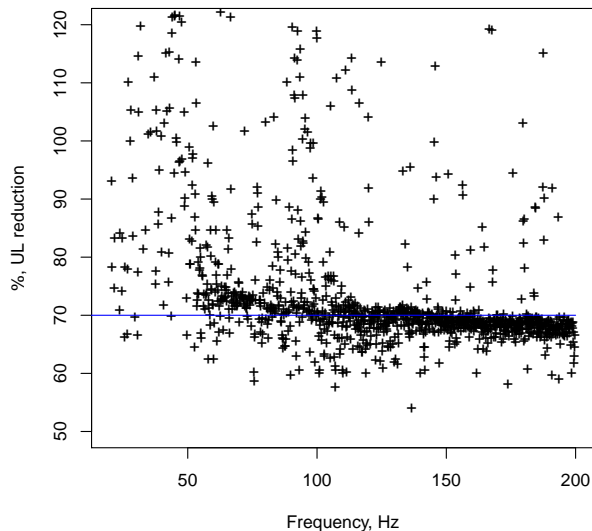


FIG. 2. Ratio of the loosely coherent worst-case upper limit (this search) compared to worst-case upper limit from the PowerFlux search[8]. (color online)

upper limits are obtained by maximizing upper limits established for individual sky locations, spindowns and frequency bands. Therefore, they are applicable to any subset of searched parameter space.

The population average proxy upper limits are computed as weighted average of upper limits from individual polarizations. This procedure is comparable to computing scaled background level as done by other all-sky searches [7–9].

To provide true population average upper limit in every frequency band one would need to verify the proxy by performing injections in every frequency band. This is not practical as the amount of computation would be larger than the actual search. Instead we verify our proxy by performing 1440 injections in the entire 20–200 Hz range, uniformly distributed in frequency. The uniform distribution was chosen to sample the full variety of detector artifacts. Sky location and orientation of the source was also chosen uniformly. The spindown was between -7.5×10^{-10} and -2.3×10^{-11} Hz/s uniformly distributed in logarithm of absolute value.

	Worst-case Circular		Population average
Depth	24.5	70.0	30.7
Depth error	6.5	16.5	8.4

TABLE I. Sensitivity depth

Achieved sensitivity depth [13]. The large error is due to combs of instrumental lines.

For each injection the analysis was carried out just

as it was done in the real search, including outlier followup. An injection was considered detected if there was an outlier in the final outlier table within $50 \mu\text{Hz}$ of the true injection frequency f_0 , within 2.5×10^{-11} Hz/s of true injection spindown and within $1.5 \text{ Hz}/f_0$ in ecliptic distance (distance between projection of outlier and injection location from unit sphere onto the ecliptic plane).

For injections above 50 Hz the detection rate is 95%, while below 50 Hz the rate is 80%. The lower detection rate at low frequencies is due to heavy contamination with detector artifacts. This improves on the analysis carried out with PowerFlux algorithm [16] where non-Gaussian bands had only 75% recovery rate, when injected at the larger worst-case upper limit level.

The search pipeline was previously described in [3]. For this analysis we start with a coherence length of 4 hours (Table III). Fewer stages are used compared to [3], while maintaining the 3-day coherence length of the final stage. The minimum SNR of outliers from the final stage was increased to 17. Results of testing population average proxy show the cutoff allows to recover 95% of signals above 50 Hz.

Full list of outliers detected in the search is available in [14]. Table II shows a summary of that list. The summary excludes all outliers within 0.01 Hz of multiples of 0.5 Hz, which are induced by 0.25 Hz combs of instrumental lines [8]. The remaining outliers are summarized by displaying the largest SNR outlier for each 0.1 Hz band.

The top 5 outliers are caused by hardware injected simulated signals whose parameters are listed in Table IV. The rest are due to large hardware artifacts.

Figure 3 presents circular polarization upper limits converted into maximum range curves [8, 9]. At the high end of the frequency range we are sensitive to a source with 10^{-6} equatorial ellipticity up to 440 pc away. It is known that neutron stars can readily support equatorial ellipticities of more than 10^{-6} [17, 18].

Boson condensates around black holes are another potential source of gravitational waves [19–21]. As an example, we include a figure showing the detection range for vector boson condensate with parameter $\alpha = 0.03$ around black holes with spin 0.2. The upper limit data [14] includes a separate set of upper limits covering near 0 frequency derivatives.

The search was performed on the ATLAS cluster at AEI Hannover, for which we thank Bruce Allen. We also thank Carsten Aulbert and Henning Fehrmann for their support.

This research has made use of data, software and/or web tools obtained from the LIGO Open Science Center (<https://losc.ligo.org>), a service of LIGO Laboratory, the LIGO Scientific Collaboration and the Virgo Collaboration. LIGO is funded by the U.S. National Science Foundation. Virgo is funded by the French Centre National de Recherche Scientifique (CNRS), the Italian Istituto Nazionale della Fisica Nucleare (INFN) and the

Idx	SNR	Frequency Hz	Spindown nHz/s	RA _{J2000} degrees	DEC _{J2000} degrees	Description
1	870	52.80832	0.006	306.634	-83.997	Hardware injection ip5
2	637	191.03126	-8.652	351.425	-33.552	Hardware injection ip8
4	387	146.16934	-6.710	359.608	-65.199	Hardware injection ip6
5	376	38.47793	-6.235	332.323	-14.679	Hardware injection ip12
6	300	108.85718	-0.006	178.641	-33.400	Hardware injection ip3
22	54	99.97667	-5.115	100.314	-41.321	coincident contamination in LHO and LLO
23	50	31.51238	-5.619	226.702	-23.180	Heavy contamination, 0.25 Hz comb in H1, 31.512 Hz line in L1
33	27	65.51035	-5.419	198.120	-40.763	0.25 Hz comb of instrumental lines
36	23	32.69785	-9.940	45.757	-37.300	Lack of coherence, contamination in H1
38	21	82.51584	-3.994	157.388	-46.681	Lack of coherence, 0.25 Hz comb in H1
39	21	81.52983	-6.310	332.731	-45.648	0.25 Hz comb of instrumental lines
40	21	107.13643	-6.677	12.094	-57.316	coincident artifacts at 107.12 Hz in H1 and L1
42	20	113.01128	1.044	304.688	9.253	0.25 Hz comb of instrumental lines
45	19	90.65642	-6.944	302.827	59.828	no coherence, disturbed H1 spectrum
46	19	62.80672	-7.985	276.491	-12.515	Sharp bin-centered line in L1 at 62.8 Hz
47	19	45.01809	-1.227	186.589	28.604	Lines in H1 and L1 at 45 Hz, contaminated spectrum
48	18	133.30755	-6.548	124.281	-50.348	Line in L1 at 133.33 Hz
49	18	49.96416	-9.906	335.191	-18.085	Highly contaminated spectrum
50	18	164.68348	-4.927	48.010	-9.672	Line in L1 at 164.7 Hz
51	18	86.51503	-5.252	56.836	-36.012	Coincident lines at 86.5 Hz, 0.25 Hz comb, sloping spectrum in L1
52	18	48.98773	-4.410	43.189	-22.949	Highly contaminated H1 and L1 spectrum near 49 Hz
53	18	192.83187	-7.790	248.222	46.044	Contaminated H1 spectrum
56	18	54.12124	-9.790	225.480	-16.962	Sharp bin-centered line in L1 at 54.1 Hz
57	17	91.71446	-8.506	128.301	-28.413	Disturbed spectrum in H1 and L1
58	17	53.93050	-2.956	212.788	-24.064	Disturbed H1 spectrum
59	17	107.66022	-9.660	24.618	-6.139	Sharp line in L1 at 107.7 Hz

TABLE II. Outliers that passed detection pipeline excluding outliers within 0.01 Hz from 0.25 Hz comb of instrumental lines. Only the highest-SNR outlier is shown for each 0.1 Hz frequency region. Outliers marked with “line” had strong narrowband disturbances identified near the outlier location. Frequencies are converted to epoch GPS 1130529362.

Stage	Coherence length (hours)	Minimum SNR
0	4	8
1	4	8
2	8	9
3	24	10.5
4	72	17

TABLE III. Simulation parameters

Parameters of 5-stage pipeline used for analysis. Stage 1 uses finer grid spacing and serves to narrow down outliers for subsequent analysis. Stage 4 outliers are subjected to consistency check between interferometers.

Label	Frequency Hz	Spindown nHz/s	RA _{J2000} degrees	DEC _{J2000} degrees
ip3	108.857159	-1.46×10^{-8}	178.37257	-33.4366
ip5	52.808324	-4.03×10^{-9}	302.62664	-83.83914
ip6	146.169370	-6.73×10^0	358.75095	-65.42262
ip8	191.031272	-8.65×10^0	351.38958	-33.41852
ip10	26.341917	-8.50×10^{-2}	221.55565	42.87730
ip11	31.424758	-5.07×10^{-4}	285.09733	-58.27209
ip12	38.477939	-6.25×10^0	331.85267	-16.97288

TABLE IV. Parameters of the hardware-injected simulated continuous wave signals during the O1 data run (epoch GPS 1130529362). Because the interferometer configurations were largely frozen in a preliminary state after the first discovery of gravitational waves from a binary black hole merger, the hardware injections were not applied consistently. There were no injections in the H1 interferometer initially, and the initial injections in the L1 interferometer used an actuation method with significant inaccuracies at high frequencies.

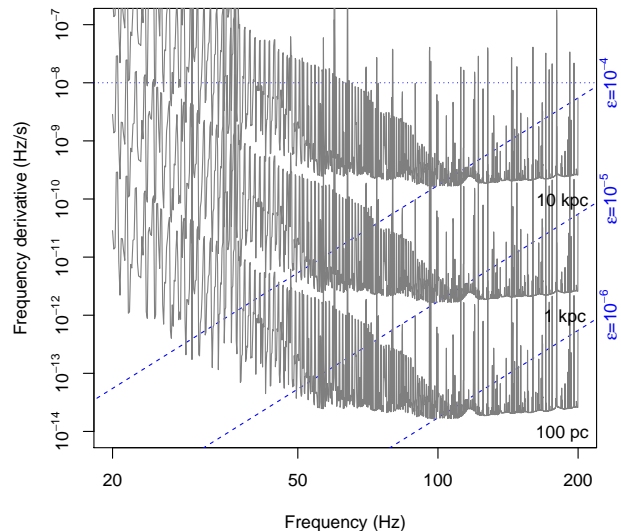


FIG. 3. Range of the search for neutron stars spinning down solely due to gravitational radiation. This is a superposition of two contour plots. The grey and red solid lines are contours of the maximum distance at which a neutron star could be detected as a function of gravitational wave frequency f and its derivative \dot{f} . The dashed lines are contours of the corresponding ellipticity $\epsilon(f, \dot{f})$. The fine dotted line marks the maximum spindown searched. Together these quantities tell us the maximum range of the search in terms of various populations [8, 9] (color online).

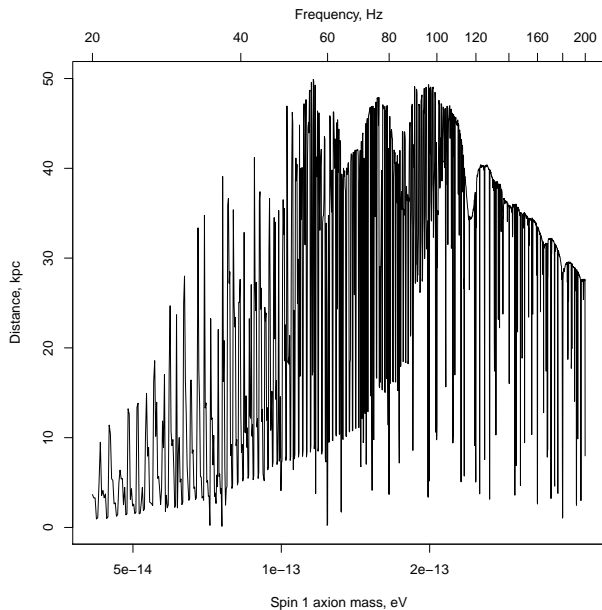


FIG. 4. Sensitivity range to signals from vector boson condensates with parameter $\alpha = 0.03$ around black holes with spin 0.2. This plot was produced using worst-case near-0 spin-down upper limits.

Dutch Nikhef, with contributions by Polish and Hungarian institutes.

^a vladimir.dergachev@aei.mpg.de

^b maria.alessandra.papa@aei.mpg.de

- [1] On blind searches for noise dominated signals: a loosely coherent approach, V. Dergachev, *Class. Quantum Grav.* **27**, 205017 (2010).
- [2] Loosely coherent searches for sets of well-modeled signals, V. Dergachev, <https://arxiv.org/abs/1807.02351> arXiv:1807.02351
- [3] Loosely coherent searches for medium scale coherence lengths, V. Dergachev, *Phys. Rev. D* **85**, 062003 (2012)
- [4] LIGO Open Science Center, <https://losc.ligo.org>
- [5] Advanced LIGO, J. Aasi *et al.* (LIGO Scientific Collaboration), *Class. Quantum Grav.* **32** 7 (2015)
- [6] M. Vallisneri *et al.* "The LIGO Open Science Center", proceedings of the 10th LISA Symposium, University of Florida, Gainesville, May 18-23, 2014, arXiv:1410.4839
- [7] First low-frequency Einstein@Home all-sky search for continuous gravitational waves in Advanced LIGO data, B. P. Abbott *et al.* (LIGO Scientific Collaboration and Virgo Collaboration), arXiv:1707.02669 [gr-qc], submitted to *Phys. Rev. D*
- [8] All-sky Search for Periodic Gravitational Waves in the O1 LIGO Data, B. P. Abbott *et al.* (LIGO Scientific Collaboration and Virgo Collaboration), *Phys. Rev. D* **96**, 062002 (2017)
- [9] Full Band All-sky Search for Periodic Gravitational Waves in the O1 LIGO Data, B. P. Abbott *et al.* (LIGO Scientific Collaboration and Virgo Collaboration), *Phys. Rev. D* **97** 102003 (2018).
- [10] Hough transform search for continuous gravitational waves, B. Krishnan, A. M. Sintes, M. A. Papa, B. F. Schutz, S. Frasca, and C. Palomba *Phys. Rev. D* **70**, 082001 (2004)
- [11] Search for continuous gravitational waves: Optimal StackSlide method at fixed computing cost, R. Prix and M. Shaltev *Phys. Rev. D* **85**, 084010 (2012)
- [12] Identification and mitigation of narrow spectral artifacts that degrade searches for persistent gravitational waves in the first two observing runs of Advanced LIGO, P.B. Covas *et al.* (LSC Instrument Authors) *Phys. Rev. D* **97**, 082002 (2018)
- [13] Fast and Accurate Sensitivity Estimation for Continuous-Gravitational-Wave Searches, C. Dreissigacker, R. Prix, K. Wette, *Phys. Rev. D* **98**, 084058 (2018)
- [14] See EPAPS Document No. [number will be inserted by publisher] for numerical values of upper limits.
- [15] A Novel Universal Statistic for Computing Upper Limits in Ill-behaved Background, V. Dergachev, *Phys. Rev. D* **87**, 062001 (2013).
- [16] Comprehensive All-sky Search for Periodic Gravitational Waves in the Sixth Science Run LIGO Data J. Aasi *et al.* (LIGO Scientific Collaboration and Virgo Collaboration), *Phys. Rev. D* **94**, 042002 (2016).
- [17] Breaking Strain of Neutron Star Crust and Gravitational Waves, C. J. Horowitz and K. Kadau, *Phys. Rev. Lett.* **102**, 191102 (2009).
- [18] Maximum elastic deformations of relativistic stars, N. K. Johnson-McDaniel and B. J. Owen, *Phys. Rev. D* **88**, 044004 (2013)
- [19] Black Hole Superradiance Signatures of Ultralight Vectors, M. Baryakhtar, R. Lasenby, M. Teo, *Phys. Rev. D*

- 96**, 035006s
- [20] Black Hole Mergers and the QCD Axion at Advanced LIGO, A. Arvanitaki, M. Baryakhtar, R. Lasenby, S. Dimopoulos, S. Dubovsky, Phys. Rev. D **95**, 043001
- [21] Discovering the QCD Axion with Black Holes and Gravitational Waves, A. Arvanitaki, M. Baryakhtar, X. Huang, Phys. Rev. D **91**, 084011